Effect of heat treatment on mechanical properties and microstructure of selective laser melting 316L stainless steel

Effect of heat treatment on mechanical properties and microstructure of selective laser melting 316L stainless steel

M S I N Kamariah[1*], W S W Harun[2], N Z Khalil[2], F Ahmad[3], M H Ismail[4], S Sharif[5]

[1]Institute of Postgraduate Studies, Universiti Malaysia Pahang, Lebuhraya Tun Razak, 26300 Gambang, Kuantan, Pahang, Malaysia.
[2]Green Research for Advanced Materials (Gramslab), Human Engineering Group, Faculty of Mechanical Engineering, Universiti Malaysia Pahang, 26600 Pekan, Pahang, Malaysia.
[3]Department of Mechanical Engineering, Universiti Teknologi PETRONAS, Malaysia.
[4]Faculty of Mechanical Engineering Universiti Teknologi MARA, Shah Alam, Selangor, Malaysia.
[5]Department of Materials, Manufacturing & Industrial Engineering, Faculty of Mechanical Engineering, Universiti Teknologi Malaysia.

*Corresponding author: nurul.kamariah01@gmail.com

Abstract. Selective Laser Melting (SLM) has been one of the preferred Additive Manufacturing process to fabricate parts due to its merits in terms of design freedom, lower material waste and faster production when compare to the conventional manufacturing processes. However, due to the thermal gradient experienced during the process, the parts are exposed to the residual stress that leads to parts distortion. This work presents the effect of heat treatments on the micro-hardness of 316L stainless steel parts. In current study, SLM has been employed to fabricate 316L stainless steel compacts. Different heat treatments of 650°C, 950°C, and 1100°C for 2 hours were applied on the compacts. Hardness test were performed on the as-built and heat-treated compacts. The relationship between the microstructures and micro-hardness were discussed in this paper. The results revealed that the micro-hardness of the as-built compacts is between 209.0 and 212.2 HV, which is much higher than the heat-treated compacts.

1. Introduction

Selective Laser Melting (SLM) is the frequently adopted additive manufacturing technology that use powdered raw material that is melted by a high energy focused laser prior to its consolidation. The low material waste, high geometrical freedom in design, and faster production of parts are its main strength when compared to the conventional manufacturing methods [1]. The excellent mechanical properties which are comparable or better than those of the casted counterparts are another credit of this method.

The effectiveness of SLM fabrication method also rely on the design parameters, for examples, the building orientation of parts, and the scanning patterns or strategy [1, 2]. Nevertheless, the design parameters can be restricted by the SLM machine such as the size of the parts. Building orientation will alter the build schedule of the SLM process. Therefore, different building orientations of parts will cause the parts to experience different thermal history [3, 4]. However, the rapid heating and cooling experienced by a part during its fabrication lead to high temperature gradient that generates residual stresses which cause part distortion [5]. This will detrimentally give impact on the mechanical behaviour of fabricated parts [6].

316L stainless steel has been broadly study for SLM [7]. This is due to the widespread application of this material in various industry, as it exhibits outstanding corrosion resistance and excellent ductility [8]. Therefore, its applications can be found in the fields of biomedical, aerospace, automotive, and marine. Some of the research done has shown the ability of SLM to improve the mechanical properties of parts when compare to conventional methods. This includes the study done by Yadroitsev et al where they observed nearly 50% increase of yield stresses of fabricated 316L SLM parts compare to forging and 20-30% of elongation of the forging [9].

The mechanical properties of the SLM fabricated parts are strongly influenced by the grain structure of molten pool [10]. Besides that, cellular dendrites are exhibited at the microstructure after SLM process due to high thermal gradient and high cooling rate [10]. The cell orientations are likely towards the gradient inside the melting pool [11, 12]. In terms of mechanical properties, Sun et. al. work managed to achieve high micro-hardness value compare to the annealed 316L stainless steel counterpart [7]. It is believed that this result is influenced by the nano-scale amorphous inclusions quantity and the dislocation density.

It will be beneficial if the 316L stainless steel parts could be used directly after SLM fabrication or heat-treated if the mechanical properties are satisfied. Therefore, it is necessary to understand the relationship between microstructure and the mechanical performance of the as-built and the heat treated samples. This study aims to understand heat treatment effect on micro-hardness of 316L stainless steel compact fabricated by SLM.

2. Experimental Procedure

Gas-atomised 316L stainless steel (SS) powder provided by SLM GmbH with mean powder particle size of 30 μm was utilised in this research. The powder particle morphology is as shown in Figure 1. Mainly, spherical-shaped particles with some smaller satellite particles attached can be observed. The chemical composition of the as-received powder is shown in Table 1. SLM of dog-bone compacts were accomplished via an 125HL SLM with 400W YLR Faber laser. All compacts were fabricated under Argon atmosphere to preclude oxidation. The dimension of the dog-bone compacts is shown in Figure 2. The compacts were fabricated with different building orientation depicted in Figure 3. Table 2 summarised the processing parameters utilised in this research.

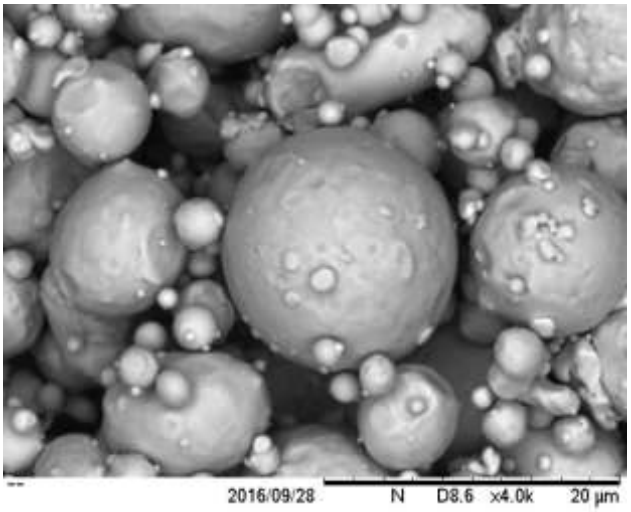

Figure 1. SEM image of as-received 316L SS particle powder morphology.

Table 1. Chemical compositions (weight %) of the as-received 316L stainless steel powder.

Element (wt.%)	Fe	Cr	Ni	Mo	Mn	Si	P	S	C
316L SS	Bal.	16.8	10.4	2.1	1.11	0.56	0.03	0.011	0.01

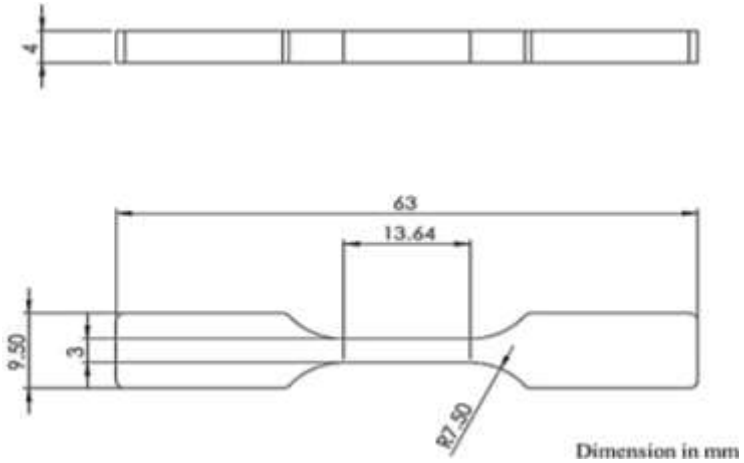

Figure 2. Detailed dimensions of tensile compacts based on ASTM E8 standard.

Identified process parameters were used to fabricate compacts at different angles of building orientation of compacts from building platform at 0°, 45°, and 90°, as shown in Figure 3. Each compact experienced same build schedule which can be consider as one single job as they were processed simultaneously, and cooling-heating rates during fabrication. Referring to Figure 3, three different axis are illustrated which represent building direction (BD), scanning direction (SD), and transverse direction (TD). For the microstructure study, the compacts were cross-sectioned at the BD and SD planes at the dotted-red box region.

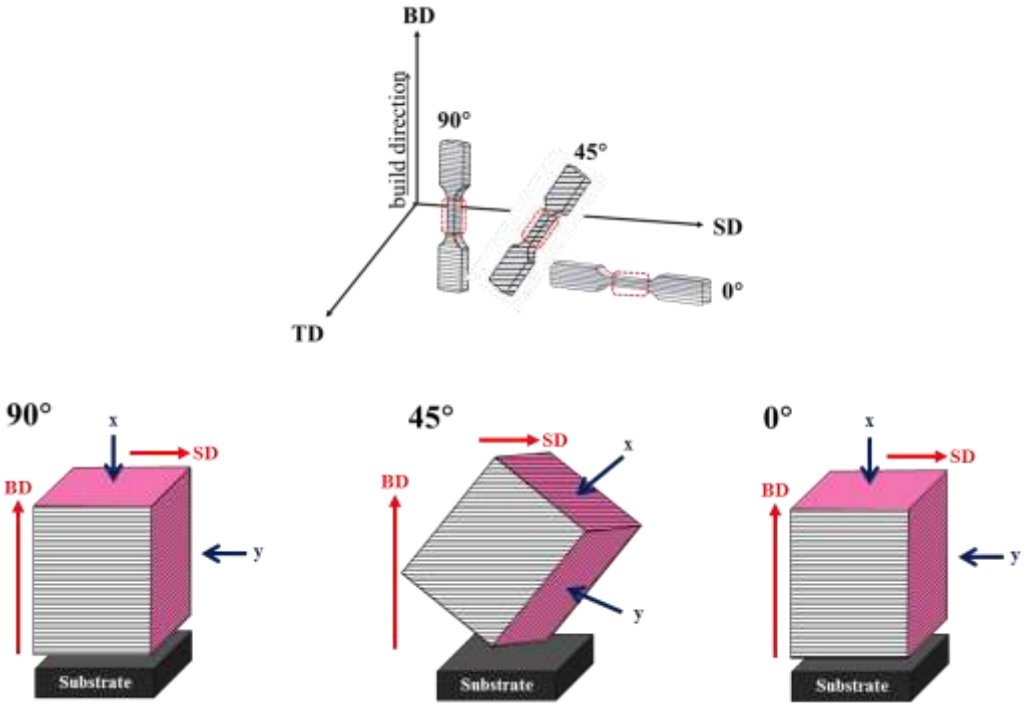

Figure 3. Schematic of compact positioning during SLM fabrication process.

Table 2. Process parameters utilised for 316L SS SLM compacts fabrication.

Laser Power (W)	Scanning speed (mm/min)	Layer thickness (μm)	Platform temperature (°C)	Argon gas consumption in operation (mL/min)
200	800	30	150	1.2

After fabrication, the compacts were detached from the build substrate. A total of twelve different conditions of 316L SS were taken into account. The "as-built" (AB) condition is referred to the untreated SLM samples. Some of the compacts from each building orientation were subjected to heat treatment (HT) using a horizontal tube furnace under argon gas with 10°C min^{-1} of heating rate. The heat treatment process were conducted at three difference temperature which are 650°C, 950°C, and 1100°C for 2 hours and were furnace cooled. Table 3 summarized the heat treatment conditions employed.

Table 3. Heat treatment condition to SLMed 316L stainless steel compacts.

Compact	**Heat treatment cycle**
As-Built	No heat treatment
HT1	650°C for 2 hours, furnace cooling
HT2	950°C for 2 hours, furnace cooling
HT3	1100°C for 2 hours, furnace cooling

The compacts were grinded, polished, and chemically etched for 5 minutes using solution of 7.5 ml nitric acid, 5.0 ml hydrofluoric acid, and 37.5 mL distilled water. The microstructures were analysed using optical microscopy (OM) (OLYMPUS BX51M).

Vickers micro-hardness tester (MATSUZAWA Type MMT X7) were utilised to conduct hardness measurements on the surface of mounted compacts under a 0.5 kg load for 10 s of dwell time. Diamond indenter was used with five repetitions per compacts.

3. Results and Discussion

The results of the Vickers hardness (HV) testing were evaluate through: (i) comparing SLM compacts hardness values for different heat treatment conditions; and (ii) comparing SLM compacts values for different building orientations.

Table 4. Results of average hardness values (HV) for SLMed 316L stainless steel compacts based on different conditions.

Sample	Building orientation (°)	Heat treatment cycle	Hardness (HV)
0-AB	0	-	209.0
45-AB	45	-	212.2
90-AB	90	-	212.0
0-HT 1	0	650°C for 2 hours, furnace cooling	201.8
45-HT 1	45	650°C for 2 hours, furnace cooling	215.5
90-HT 1	90	650°C for 2 hours, furnace cooling	204.0
0-HT 2	0	950°C for 2 hours, furnace cooling	181.7
45-HT 2	45	950°C for 2 hours, furnace cooling	186.0
90-HT 2	90	950°C for 2 hours, furnace cooling	191.5
0-HT 2	0	1100°C for 2 hours, furnace cooling	173.3
45-HT 2	45	1100°C for 2 hours, furnace cooling	185.7
90-HT 2	90	1100°C for 2 hours, furnace cooling	170.8

In Figure 4, the values of hardness are plotted against the building orientation angles (0°, 45°, 90°) from SLM build substrate plate for all four heat treatment conditions of compacts. Note that each data point that poses the hardness value is the average values of six micro-hardness measurements taken at the cross-sectioned parts at x and y, i.e. BD and SD planes, of the compacts, significantly. Thus, represents the average hardness values of the specific compact conditions.

It can be seen in Figure 4, the as-built and each heat treated conditions shows different trend of hardness values. Referring to 0° and 45° building orientations, the as-built and HT1 compact conditions shows similar variation of the hardness values. Although there are differences between the average hardness values of 90° building orientation for as-built compact, i.e. 212.0 HV, and HT1 compact, i.e. 204.0 HV, the range of values distribution shows that the difference is small. Thus, it can be said that hardness values gain for as-built condition is similar to HT1 compact condition. Nevertheless, the HT2 and HT3 compact conditions exhibit significant lower hardness values than as-built and HT1 compact conditions. This finding is aligned with the results gain by Sistiaga et. al. at similar HT3 compact condition that marked the beginning of the lower hardness values of the SLMed heat treated compact condition compare to the as-built and other lower heat treatment temperature [13]. HT2 and HT3 compact conditions illustrates dissimilar pattern of hardness values. 0° building orientation for HT2 shows a slightly higher than HT3 compact condition. However, a more significant difference can be seen for 90° building orientation, where HT2 shows an average value of 191.5 HV

which is higher compare to the lower average value of 170.8 HV for HT3. However, the values gained for 45° building orientation for HT2 and HT3 are similar.

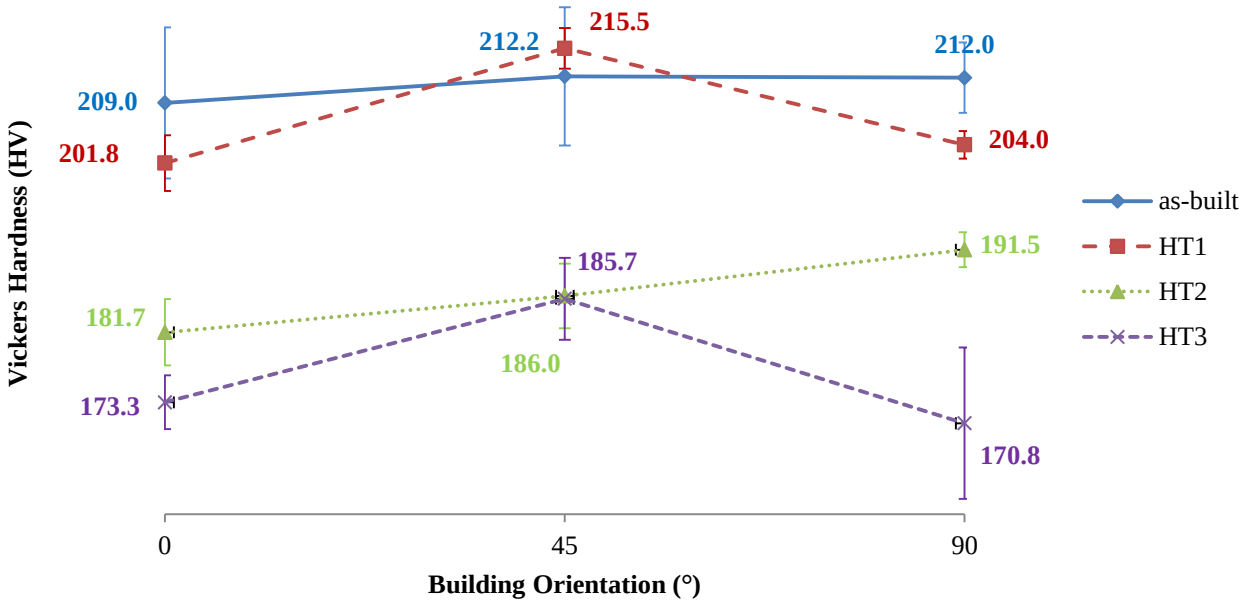

Figure 4. Average micro-hardness (HV) values for SLM compacts.

The microstructure was observed using optical microscope (OM) to identify the cellular dendrites structures, and the phase formation of austenite and ferrite on the compacts from each compact condition, i.e. at different heat treatment conditions.

Figure 5 (a) and (b) shows the structure of melt pools and fine cellular dendrites microstructure in the SLM-ed compacts for as-built and HT1 conditions. This microstructure is a general characteristics poses by metal materials manufactured through AM process as the consequences of the rapid solidification rates of a local melted region, precisely laser-scanned areas. This is typical for area that exposed to short laser-material interaction time during build process [14]. The high hardness value gained for as-built and HT1 conditions compare to HT2 and HT3 conditions are believed cause by the fine-grain microstructures, hence results in higher dislocation density of austenite cells [15]. This makes it difficult for slip motion along the grain boundaries, hence increases its strength and resistance towards deformation. Interestingly, as the compacts were heat treated up to a higher temperature of 950°C and 1100°C, the cellular dendrites microstructure was no longer can be observed, and the melt pool boundaries seems to be dissolved. This is the reason for low hardness value gained for HT2 and HT3 compact conditions.

The dispersion of two different iron based phases comprising of dominant face-centred cubic (FCC) structure of austenitic (γ) phase, and less prevalent body-centred cubic (BCC) structure of ferrite (δ) phase are reveal in Figure 5 (c) and (d). Material with full austenite can be gained at equilibrium according to the chemical composition of 316L stainless steel. However, some δ-ferrite formation is found due to the fast solidification and the existence of chemical elements conducive for ferrite formations which are Si, Cr, and Mo [4, 16]. Comparing Figure 5 (c) and (d), the δ-ferrite phase's volume fraction (darker phase) is slightly bigger in Figure 5 (c) than in Figure 5 (d). Hence, demonstrates that the employment of heat treatment greatly effect in the decrease of volume fraction

of δ-ferrite phase. It is known that the mechanical properties of materials are significantly affected by the volume fraction of δ-ferrite phase.

Referring to Figure 4, the micro-hardness values of HT3 for 0° and 90° building orientations are the lowest follows by HT2, and HT1 significantly. These are the result of the enforcement of microstructural coarsening enforced through the process of heat treatment. Note that a room temperature, the δ-ferrite phase is harder compare to the austenitic phase. Therefore, reducing the δ-ferrite phase during heat treatment will lead for the lower hardness values gained. This is supported by the research done by Yadollahi et. al [4, 17, 18].

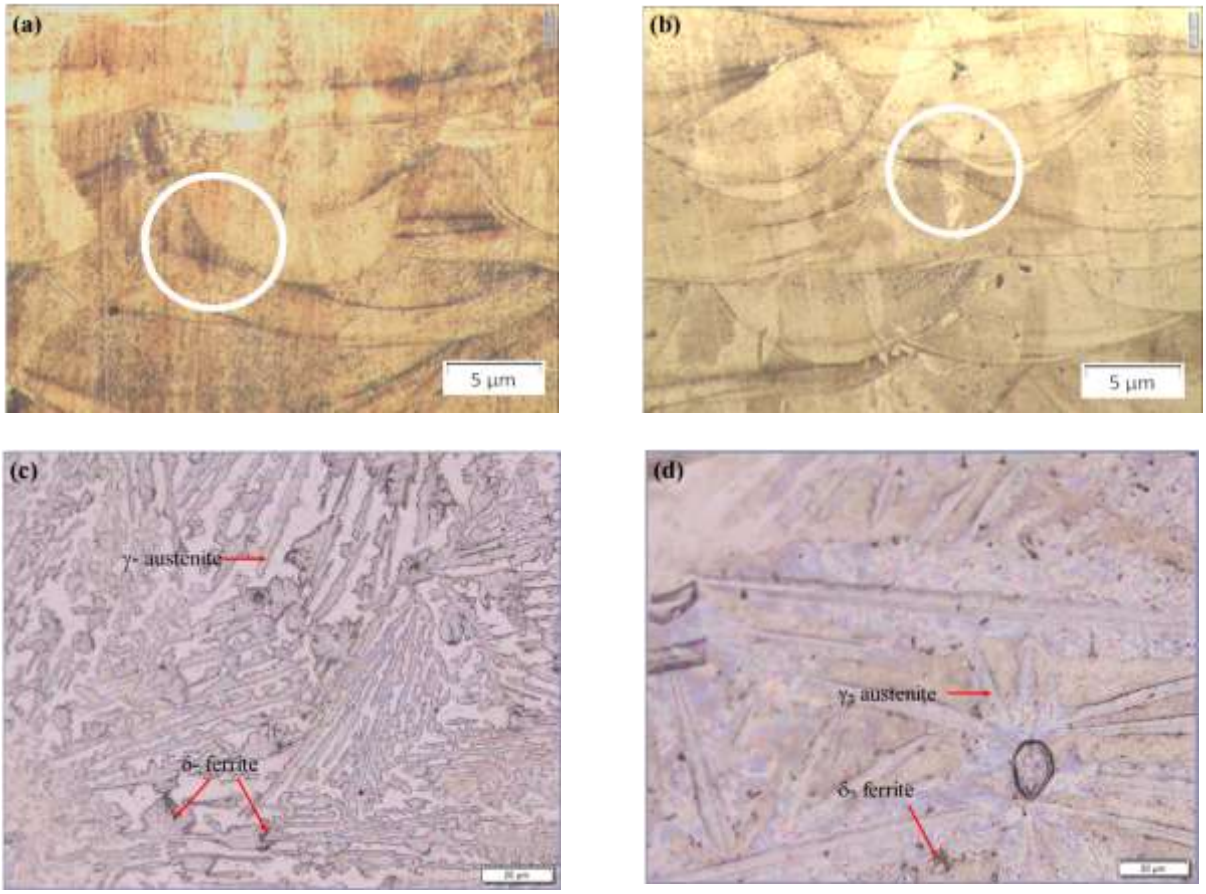

Figure 5. Optical microscope image of BD plane cross-sectioned 316L stainless steel compacts produced by SLM. (a) As-built, (b) HT1, (c) HT2, and (d) HT3 conditions.

Noted that Figure 6 represents the micro-hardness values were taken only at the 'y' cross-sectioned plane of the SD plane of the compacts plotted against the building orientation. Figure 6 reveals the variation of the micro-hardness vales for different building orientation. For as-built, HT1, and HT3 conditions, the lowest micro-hardness values are at the 0° building orientation, follows by the 90° building orientation. Both 0° building orientation and 90° building orientation show variation in the values. 45° building orientation on the other hand exhibits the highest micro-hardness values for those three conditions, i.e. as-built, HT1, and HT3, but with a much stable values. A different trend is shown by HT2 where the micro-hardness measurements increase with the increase of degree of building orientation. However, the average value gains for 0° building orientation, i.e. 181 HV, and 45° building orientation, i.e. 184 HV, do not show a significant different.

The micro-hardness variation of each orientation demonstrates anisotropy in SLM as reported in other literatures [14, 19]. This is a usual quality of additive manufacturing processes for metal parts [20]. This is believed due to the localised melting of powder particles that leads to non-homogeneous morphologies [14]. Besides that, it is also caused by the layer-by-layer approaches and the formation

of grain structures and textures due to the thermal gradient [21]. The variations of micro-hardness values of 0° building orientation is probably due to the existence of high residual stresses. This phenomenon might be due to inhomogeneity of delivered powder layer which causes differences in layers' thicknesses caused by the roughness of the substrate and non-parallel between coater and the substrate. This leads to strains during cooling. Deformations and loss of the metallurgical contact with the substrate during manufacturing as observed during the fabrication 0° building orientation resulted in accumulation of heat as well as occurrence of redistribution of stresses. As for 45° building orientation, the micro-hardness values measured are more stable. During the fabrication, the compact experienced more layer-by-layer formation as compared to 0° building orientation's compact. During the process, powders are melted and solidification occurs under high laser energy. Thus, heat is conducted layer-by-layer in the compact. For each layer fabrication, the compact is contacted to support structures, and hence, helps as heat conductor by transferring the heat away from the working compact. As a result of the heat dissipation, the influence from residual stresses on the process is fairly stable. In contrast to 45° building orientation's compacts, the 90° building orientation's compacts have shown a variation in their micro-hardness values probably due to the existence potential of high residual stresses that mainly oriented along the building direction. This phenomenon is also aligning with other reported literatures [22-24]. As for real building application, parts with more consistence microhardness property and low residual stress potential is more preferable as shown by 45° building orientation in this study.

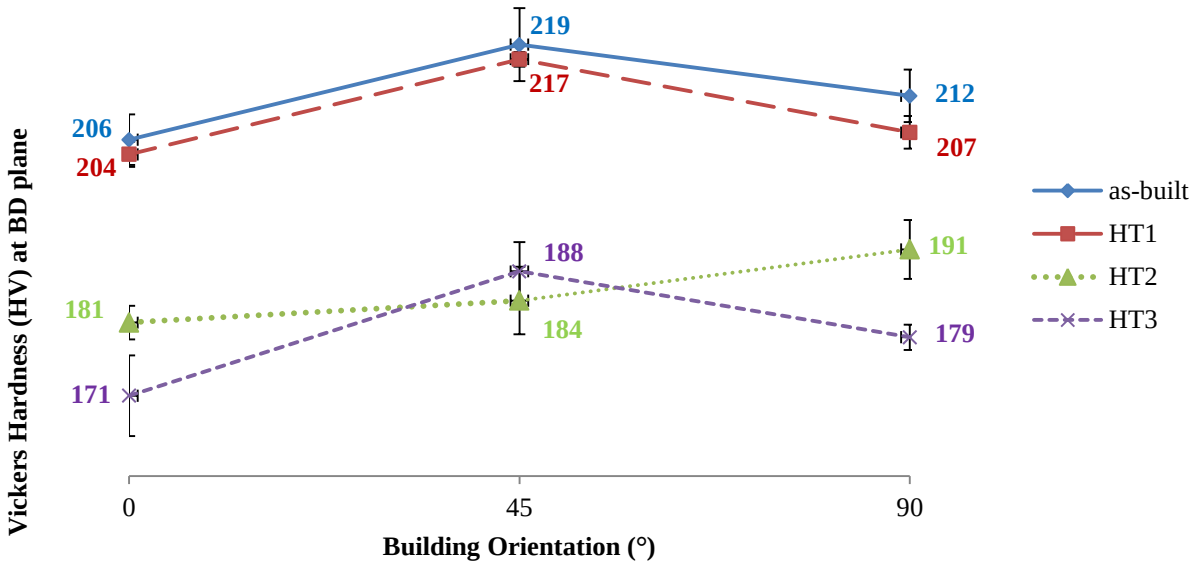

Figure 6. Average micro-hardness (HV) values for at BD plane cross-sectioned of SLM compacts.

4. Conclusions

This research concludes the following points,

1) The results reveal that the micro-hardness of the as-built compacts is between 209.0 and 212.2 HV, which is much higher than the heat-treated compacts. Heat treatment causes the hardness values of the SLM -fabricated 316L stainless steel compacts to decrease. The lowest hardness value gain was for the highest heat treatment temperature tested is 171 HV for 1100 °C with 2 hours soaking time.
2) Mechanical properties of SLM-produced 316L stainless steel are affected by the formation of fine cellular dendrites microstructures and heat treatment. The fine cellular dendrites of completed parts due to localized melting of powder and rapid heating-and-cooling rates during SLM fabrication.

Thus, leads to high micro-hardness values gained of the SLMed parts. While heat treatment reduced the volume fraction of δ-ferrite and become the reason for the lower micro-hardness values gained in the study.

3) Variation of micro-hardness values for different building orientations demonstrates anisotropy properties of the SLM fabricated compacts. This is due to the non-homogeneous morphologies of melted powder particles, and thermal gradient of the built compacts. The inconsistency hardness values of compacts for 0° and 90° building orientations are probably due to the high residual stresses existed in the compacts.

Future studies would be done to excess the existence of residual stress for building orientations conditions and their effects on other mechanical properties, and deeper microstructure study.

Acknowledgments
Authors would like to recognise the contributions of Universiti Malaysia Pahang (Grant no. RDU151314, RDU160354, GRS1503121), the Human Engineering Group (HEG), and Universiti Malaysia Pahang for its comprehensive facilities support in this research.

References

[1] Zhang B, Dembinski L and Coddet C 2013 The study of the laser parameters and environment variables effect on mechanical properties of high compact parts elaborated by selective laser melting 316L powder *Materials Science and Engineering: A* **584** 21-31
[2] Ahmadi A, Mirzaeifar R, Moghaddam N S, Turabi A S, Karaca H E and Elahinia M 2016 Effect of manufacturing parameters on mechanical properties of 316L stainless steel parts fabricated by selective laser melting: A computational framework *Materials & Design* **112** 328-38
[3] Ma M, Wang Z and Zeng X 2017 A comparison on metallurgical behaviors of 316L stainless steel by selective laser melting and laser cladding deposition *Materials Science and Engineering: A* **685** 265-73
[4] Yadollahi A, Shamsaei N, Thompson S M and Seely D W 2015 Effects of process time interval and heat treatment on the mechanical and microstructural properties of direct laser deposited 316L stainless steel *Materials Science and Engineering: A* **644** 171-83
[5] Wang D, Yang Y, Liu R, Xiao D and Sun J 2013 Study on the designing rules and processability of porous structure based on selective laser melting (SLM) *Journal of Materials Processing Technology* **213** 1734-42
[6] Krakhmalev P, Fredriksson G, Yadroitsava I, Kazantseva N, Plessis A d and Yadroitsev I 2016 Deformation Behavior and Microstructure of Ti6Al4V Manufactured by SLM *Physics Procedia* **83** 778-88
[7] Sun Z, Tan X, Tor S B and Yeong W Y 2016 Selective laser melting of stainless steel 316L with low porosity and high build rates *Materials & Design* **104** 197-204
[8] AlMangour B, Grzesiak D and Yang J-M 2017 In-situ formation of novel TiC-particle-reinforced 316L stainless steel bulk-form composites by selective laser melting *Journal of Alloys and Compounds* **706** 409-18
[9] Yadroitsev I and Smurov I 2011 Surface Morphology in Selective Laser Melting of Metal Powders *Physics Procedia* **12** 264-70
[10] Wang D, Song C, Yang Y and Bai Y 2016 Investigation of crystal growth mechanism during selective laser melting and mechanical property characterization of 316L stainless steel parts *Materials & Design* **100** 291-9
[11] Yasa E and Kruth J P 2011 Microstructural investigation of Selective Laser Melting 316L stainless steel parts exposed to laser re-melting *Procedia Engineering* **19** 389-95
[12] Zhong Y, Liu L, Wikman S, Cui D and Shen Z 2016 Intragranular cellular segregation network structure strengthening 316L stainless steel prepared by selective laser melting *Journal of Nuclear Materials* **470** 170-8

[13] Montero Sistiaga M, Nardone S, Hautfenne C and Van Humbeeck J 2016 Effect of heat treatment of 316L stainless steel produced by selective laser melting (SLM)
[14] Yusuf S M, Chen Y, Boardman R, Yang S and Gao N 2017 Investigation on Porosity and Microhardness of 316L Stainless Steel Fabricated by Selective Laser Melting *Metals* **7** 64
[15] Saeidi K, Gao X, Zhong Y and Shen Z J 2015 Hardened austenite steel with columnar sub-grain structure formed by laser melting *Materials Science and Engineering: A* **625** 221-9
[16] Bouche G, Bechade J, Mathon M, Allais L, Gourgues A and Naze L 2000 Texture of welded joints of 316L stainless steel, multi-scale orientation analysis of a weld metal deposit *Journal of nuclear materials* **277** 91-8
[17] Imandoust A, Zarei-Hanzaki A, Heshmati-Manesh S, Moemeni S and Changizian P 2014 Effects of ferrite volume fraction on the tensile deformation characteristics of dual phase twinning induced plasticity steel *Materials & Design* **53** 99-105
[18] Kocijan A, Merl D K and Jenko M 2011 The corrosion behaviour of austenitic and duplex stainless steels in artificial saliva with the addition of fluoride *Corrosion Science* **53** 776-83
[19] Miranda G, Faria S, Bartolomeu F, Pinto E, Madeira S, Mateus A, Carreira P, Alves N, Silva F S and Carvalho O 2016 Predictive models for physical and mechanical properties of 316L stainless steel produced by selective laser melting *Materials Science and Engineering: A* **657** 43-56
[20] Chen L Y, Huang J C, Lin C H, Pan C T, Chen S Y, Yang T L, Lin D Y, Lin H K and Jang J S C 2017 Anisotropic response of Ti-6Al-4V alloy fabricated by 3D printing selective laser melting *Materials Science and Engineering: A* **682** 389-95
[21] Aboulkhair N T, Stephens A, Maskery I, Tuck C, Ashcroft I and Everitt N M 2015 Mechanical properties of selective laser melted AlSi10Mg: nano, micro, and macro properties. In: *Proc. of Solid Freeform Fabrication Symposium*, pp 1-30
[22] Vrancken B, Cain V, Knutsen R and Van Humbeeck J 2014 Residual stress via the contour method in compact tension specimens produced via selective laser melting *Scripta Materialia* **87** 29-32
[23] Rangaswamy P, Griffith M L, Prime M B, Holden T M, Rogge R B, Edwards J M and Sebring R J 2005 Residual stresses in LENS® components using neutron diffraction and contour method *Materials Science and Engineering: A* **399** 72-83
[24] Chlebus E, Kuźnicka B, Kurzynowski T and Dybała B 2011 Microstructure and mechanical behaviour of Ti—6Al—7Nb alloy produced by selective laser melting *Materials Characterization* **62** 488-95

Nomenclature

γ	Austenite phase
δ	Ferrite phase
0-AB	Compact condition with 0° building orientation and no heat treatment
0-HT 1	Compact condition with 0° building orientation and 650°C heat treated
0-HT 2	Compact condition with 0° building orientation and 950°C heat treated
45-AB	Compact condition with 45° building orientation and no heat treatment
45-HT 1	Compact condition with 45° building orientation and 650°C heat treated
45-HT 2	Compact condition with 45° building orientation and 950°C heat treated
90-AB	Compact condition with 90° building orientation and no heat treatment
90-HT 1	Compact condition with 90° building orientation and 650°C heat treated
90-HT 2	Compact condition with 90° building orientation and 950°C heat treated
AB	As-built
BD	Building direction
BCC	Body-centred cubic structure
C	Carbon (chemical element)
Cr	Chromium (chemical element)
FCC	face-centred cubic structure
Fe	Iron (chemical element)
HT1	Heat treatment cycle at 650°C for 2 hours with furnace cooling
HT2	Heat treatment cycle at 950°C for 2 hours with furnace cooling
HT3	Heat treatment cycle at 1100°C for 2 hours with furnace cooling
Ni	Nickel (chemical element)
Mn	Manganese (chemical element)
Mo	Molybdenum (chemical element)
P	Phosphorus (chemical element)
S	Sulphur (chemical element)
SD	Scanning direction
Si	Silicon (chemical element)
SLM	Selective Laser Melting
SS	Stainless Steel
TD	Transverse direction